

Structural Design for a Jaw Using Metamodels

IL-Kwon Bang¹, Dong-Heon Kang², Dong-Seop Han³, Geun-jo Han⁴, *Kwon-Hee Lee⁵

¹ Graduate student, Department of Mechanical Engineering, Dong-A Univ.
(E-mail: denver21@donga.ac.kr)

² Graduate student, Department of Mechanical Engineering, Dong-A Univ.
(E-mail: rkdehdgjs79@hotmail.com)

³ Contractor Professor of the BK21 Project, Department of Mechanical Engineering, Dong-A Univ.
(E-mail: dshan@donga.ac.kr)

⁴ Professor, Department of Mechanical Engineering, Dong-A Univ.
(E-mail: gjhan@daunet.donga.ac.kr)

⁵ Corresponding Author, Assistant Professor, Department of Mechanical Engineering, Dong-A Univ.,
Busan 604-714, Korea (E-mail: leekh@daunet.donga.ac.kr)

Abstract

Rail clamps are mechanical components installed to fix the container crane to its bottoms from wind blast or slip. Rail clamps should be designed to survive the harsh wind loading condition. In this study, the jaw structure that is one part of wedge-typed rail clamp is optimized, considering strength under the severe wind loading condition. According to the classification of structural optimization, the structural optimization of a jaw belongs to shape optimization. In the conventional structural optimization methods, they have difficulties in defining complex shape design variables and preventing mesh distortions. To overcome the difficulties, the metamodel using kriging interpolation method is introduced, replacing true response by approximate one. This research presents the shape optimization of a jaw using iterative kriging interpolation models and simulated annealing algorithm. The new kriging models are iteratively constructed by refining the former kriging models. This process is continued until the convergence criteria are satisfied. The optimum results obtained by the suggested method are compared with those obtained by the DOE (design of experiments) and VT (variation technology) methods built in ANSYS WORKBENCH.

Key Words: Container Crane, Rail Clamp, Jaw, Shape Optimization, Kriging, DOE, VT

1. Introduction

Recently, the Korean Peninsula has often come under the influence of strong typhoons. Since 2000, the powerful typhoons hit Korea were Prapiroon in 2000, Rusa 2002, Maemi in 2003 and Nabi in 2005. In special, Maemi, meaning cicada in Korean and bringing record-breaking 60 m/s winds, was one of the most powerful typhoon to hit Korea since weather records began collecting weather data. When the Maemi howled into the major port of Busan, 11 heavy duty shipping cranes, weighing up to 985 tons, were toppled and twisted beyond recognition. It was reported that the damage was so severe that it could take up to one year and KRW 40 billion (almost USD 42 million) to repair the cranes^{1,2}.

In response to this climate influence, the Ministry of Maritime Affairs & Fisheries in Korea strengthened the related regulations for facilities and equipments in port³. According to the amended regulations, the container crane in operating mode should resist the wind load at 40 m/s while in stowing mode at 70 m/s⁴. Compared to the former regulations, each limit speed rose 20 m/s. Thus, the structures for facilities and equipments in port should be designed, considering the harsh wind loads.

The trend now is to build the large-scale container ship such as ULCS (Ultra Large Container Ship), because trade has grown. For an example, the ULCS can manage 12,000 TEU. With this trend, the size of container crane has become larger than that of former container. The large-scale container crane justifies the

high design cost. Thus, it is important to design its components to meet the previously mentioned regulations.

As a container ship comes alongside the quay, the container crane is moved and stopped along rails to load and unload containers. This is called the operating mode. Then, the mechanical component called the rail clamp is utilized to fix the crane on the rails. If the rail clamp cannot play its role, the crane will run along a rail and bring about a huge accident. When a container crane is set to a stowing mode, the crane is fixed by stowage pin and tie-down load. Since this study focuses on the design of a jaw in the rail clamp, the loading condition is derived from the operating mode's wind load^{4,5}.

The wedge-typed rail clamp⁶ has different operating mechanisms according to three operating stages. In this research, the wedge-working stage is only considered to design a jaw since its load is the largest of three operating stages. Jaws play an important role in wedging the mechanism. The FE (finite element) method is utilized to predict the strength performance of a jaw. Furthermore, structural optimization scheme can be adopted to determine the optimum shape of a jaw. According to the classification of structural optimization, the structural optimization of a jaw belongs to shape optimization since its FE model is composed of solid elements. However, the conventional structural optimization methods have difficulties in defining complex shape design variables and preventing mesh distortions in the optimization process.

To overcome these difficulties, this research presents the shape optimization of a jaw using iterative kriging interpolation method

and simulated annealing algorithm. The kriging models⁷⁻¹⁰⁾ are utilized to surrogate the true models for responses. In this research, the responses mean the weight of a jaw and the maximum stress acted on a jaw. The new kriging models are iteratively constructed by refining the former kriging models. This process is continued until the convergence criteria are satisfied. The optimization problem expressed by kriging models are solved by adopting simulated annealing algorithm.

In this study, the commercial software, ANSYS/WORKBENCH¹¹⁾, is utilized to calculate the strength performance and to compare the optimum design of a jaw obtained by the suggested method.

2. FE analysis of a jaw

2.1 Mechanism of wedge-typed rail clamp^{4,6)}

Rail clamps are mechanical components installed to fix the container crane to its bottoms from wind blast or slip. As shown in Fig. 1, the number of rail clamps installed in a container crane is two. The wedge-typed rail clamp such as Fig. 2 is composed of jaw, wedge, locker, hanger, jaw pad, roller and wedge frame. Its operating mechanism is divided into three stages, which are opening stage, initial clamping stage and wedge-working stage.

The opening stage is represented as Fig. 3(a). When the locker is lifted up in the opening stage, the angle between two jaws becomes larger, and then the rail clamp is separated from the rail. Thus, this stage makes the container crane move.

Initial clamping stage in Fig. 3(b) allows both jaw pads to rail sides with small clamping force. That is, a container crane has a set position for working, fixing a container crane. This stage is operated by acting the force P . On the contrary, the wedge-working stage does not allow a container crane to move, because the clamping forces of both jaw pads increase as the wind speed increases.

The operating mechanism in the wedge-working stage is as follows: From the state of initial clamping stage, the wedge frame attached to the container crane is started to slip owing to

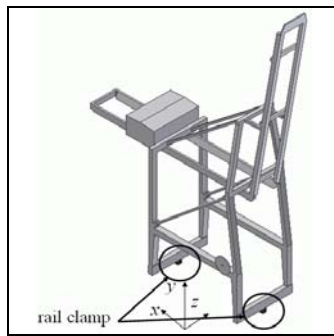


Figure 1 A container crane

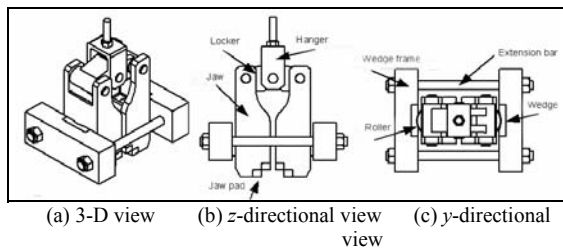


Figure 2 A container crane

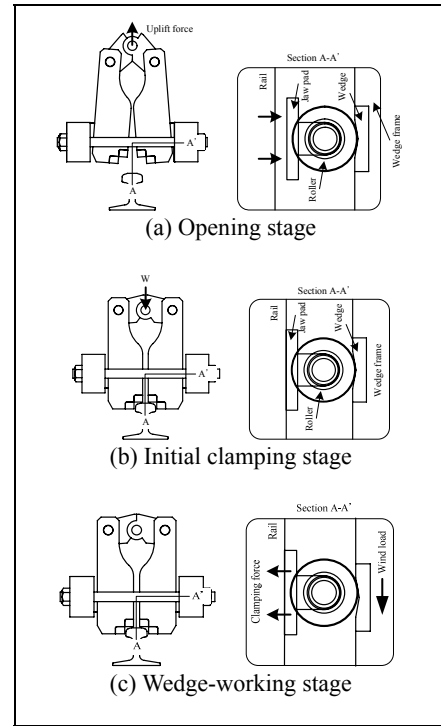


Figure 3 Operating mechanism of wedge-typed rail clamp

the increase of z -directional wind load F_z . Then, a V-shaped wedge built in the wedge frame makes a roller rotate along its slope, generating wedge action. As shown in Fig. 3(c), that results from the increase of clamping force F_p applied on each jaw pad. The clamping forces prevent a container crane from slipping along the rail. In this research, the wedge-working stage is considered to design a jaw, because it generate the largest loads of three stages.

2.2 FE model and loading and boundary conditions^{4,6)}

The regulations to design a container crane are specified in *Specification for the Design of Crane Structures* in KS, *Load Criteria of Building Structure* in Ministry of construction & Transportation (Korea), *Design Criteria of Cranes* in BS¹²⁾, etc. Since the British regulation evaluates the severest loading, this research adopted it as the load calculations.

According to the BS 2573, the z -directional wild load applied to a container crane is calculated as

$$F_z = C_{tz} \times q_h \times A_{unit} \times L \quad (1)$$

where C_{tz} and q_h are the wind load coefficients for wind load and wind pressure, and A_{unit} is the horizontal wind area per unit length, and L is the member length, respectively. By applying Eq. (1) to the container crane of Fig. 1, Eq. (1) is simplified as

$$F_z = 1.107 \times v_0^2 \quad (2)$$

where v_0 is the wind velocity. As mentioned Introduction, v_0 is set up as 40 m/s.

By the way, there are two rail clamps in a container crane and each one has two friction surfaces or two clamping surfaces. Thus, F_p is represented as

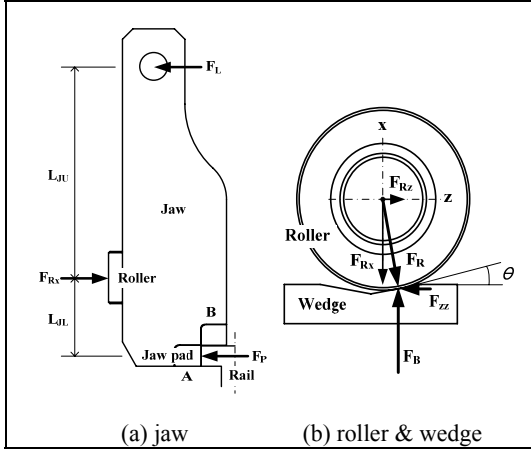


Figure 4 Free body diagram of a jaw

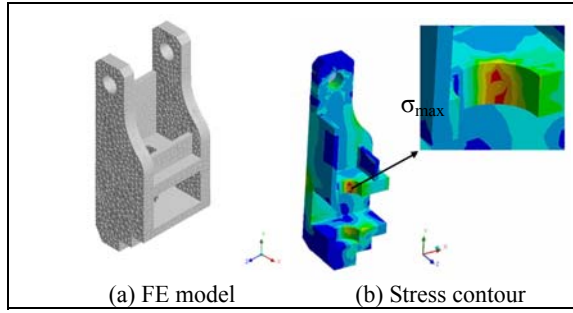


Figure 5 FE analysis of a jaw

$$F_p = \frac{F_z}{4\mu_p} \quad (3)$$

where μ_p is the friction coefficient for the contact surface between jaw pad and rail.

From the above force analysis, we can derive the forces acting on a jaw. The free body diagram of jaw can be represented as Fig. 4(a). In the wedge-working stage, F_p is generated on the jaw pads when the x -directional force of a roller F_{Rx} applies to the middle of jaw and the locker supports the top of jaw. Considering the force equilibrium in Fig. 4(a), F_L and F_{Rx} are derived as

$$F_L = \frac{L_{JL}}{L_{JU}} \cdot F_p \quad (4)$$

$$F_{Rx} = F_p + F_L = \left(1 + \frac{L_{JL}}{L_{JU}}\right) \cdot F_p \quad (5)$$

Substituting the values of F_p , L_{JL} and L_{JU} to Eq. (5), F_{Rx} is calculated as 1,110 kN. Furthermore, from the force equilibrium in Fig. 4(b), we can derive the value of F_{Rz} , and that is 197 kN. For the FE analysis of a jaw, we can assume that F_R is the external bearing load, the hole surface has fixed displacement in x direction, the surface A between jaw pad and rail has fixed displacements in x and z , and the surface B between jaw pad and rail has fixed displacement in y . Its FE model meshed with solid elements is shown as Fig. 5(a) while the stress

t_1

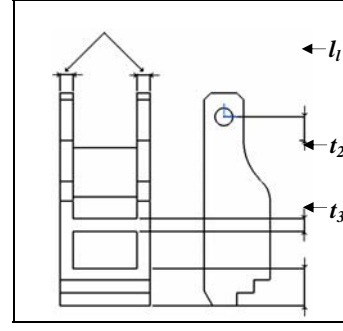


Figure 6 design variables of a jaw contour at initial design as Fig. 5(b).

3. Optimization using the kriging metamodel

3.1 Design variables and optimization formulation

The initial design satisfies the strength requirement. Thus, the weight of a jaw can be reduced by applying structural optimization. As shown in Fig. 6, in order to reduce the weight of a jaw, the design variables are set up as thicknesses of the structure (t_1 , t_2 and t_3) and length between centers of hole and curvature (l_1). In the initial design, $t_1=30.0\text{mm}$, $t_2=30.0\text{mm}$, $t_3=85.0\text{mm}$ and $l_1=54.1\text{mm}$, and its weight is 43.5kg. As shown in Fig.5(b), the maximum stress is generated at the contact area between roller and jaw, and the value is 533MPa. The material for a jaw is SCM445, and its ultimate strength is 823MPa. This value is lower than the allowable stress, considering safety factor 1.5.

Under the regulations of the Inspection Criteria for Facilities and Equipments in Port, the safety factor of a structure was set up as more than 1.5³⁾.

Theoretically, the structural optimization for a jaw can be formulated as follows:

$$\text{minimize } w(t_1, t_2, t_3, l_1) \quad (6)$$

$$\text{subject to } \sigma_i - \sigma_a \leq 0, (i=1, \dots, ne) \quad (7)$$

$$25\text{mm} \leq t_1 \leq 35\text{mm} \quad (8)$$

$$25\text{mm} \leq t_2 \leq 35\text{mm} \quad (9)$$

$$75\text{mm} \leq t_3 \leq 90\text{mm} \quad (10)$$

$$50\text{mm} \leq l_1 \leq 60\text{mm} \quad (11)$$

where w is the weight of a jaw, σ_i is the stress of i -th element, σ_a is the allowable stress, and ne is the number of finite elements. The lower and upper bounds of each design variable are determined as its minimum and maximum values not to distort the meshed finite elements.

From the looks of Eqs. (6)~(11), it looks like easy to solve the formulation. However, the structural optimization represented as Eqs. (6)~(11) belongs to shape optimization. This research utilizes the metamodel called the kriging model in lieu of true model. For this approach, Eqs. (6)~(7) are replaced by

$$\text{minimize } \hat{w}(t_1, t_2, t_3, l_1) \quad (12)$$

$$\text{subject to } \hat{\sigma}_{\max} - \sigma_a \leq 0 \quad (13)$$

where $\hat{\cdot}$ means the estimator of a response, and σ_{\max} is the maximum stress generated at the jaw. Thus, two responses are approximated, using kriging interpolation method.

3.2 Kriging interpolation method

Kriging is a method of interpolation named after a South African mining engineer named D. G. Krige, who developed the technique in an attempt to more accurately predict ore reserves. Kriging interpolation for an approximation model is well explained in Refs (7)~(10).

In the kriging model, the estimator for a true response $y(\mathbf{x})$ is represented as

$$\hat{y}(\mathbf{x}) = \hat{\beta} + \mathbf{r}^T(\mathbf{x})\mathbf{R}^{-1}(\mathbf{y} - \hat{\beta}\mathbf{q}) \quad (14)$$

where \mathbf{x} is the design variable vector, $\hat{\beta}$ is the estimated value of constant β , \mathbf{R}^{-1} is the inverse of correlation matrix \mathbf{R} , \mathbf{r} is the correlation vector, \mathbf{y} is the observed data with n_s sample data, and \mathbf{q} is the vector with n_s components of 1. In this research, $\mathbf{x} = [t_1, t_2, t_3, l_1]^T$, and y is the weight or maximum stress of a jaw. The correlation matrix and the correlation vector are defined as

$$R(\mathbf{x}^j, \mathbf{x}^k) = \text{Exp}\left[-\sum_{i=1}^n \theta_i |x_i^j - x_i^k|^2\right], \quad (j=1, \dots, n_s, k=1, \dots, n_s) \quad (15)$$

$$\mathbf{r}(\mathbf{x}) = [R(\mathbf{x}, \mathbf{x}^{(1)}), R(\mathbf{x}, \mathbf{x}^{(2)}), \dots, R(\mathbf{x}, \mathbf{x}^{(n_s)})]^T \quad (16)$$

where n is the number of design variables.

By differentiating the log-likelihood function with β and σ^2 , respectively, and setting them equal to 0, the maximum likelihood estimators of β and σ^2 are determined as Eqs. (11) and (12).

$$\hat{\beta} = (\mathbf{q}^T \mathbf{R}^{-1} \mathbf{q})^{-1} \mathbf{q}^T \mathbf{R}^{-1} \mathbf{y} \quad (17)$$

$$\hat{\sigma}^2 = \frac{(\mathbf{y} - \hat{\beta}\mathbf{q})^T \mathbf{R}^{-1} (\mathbf{y} - \hat{\beta}\mathbf{q})}{n_s} \quad (18)$$

In equations (14)~(18), \mathbf{R} , \mathbf{r} , $\hat{\beta}$ and $\hat{\sigma}^2$ are the function of the parameters θ_i ($i=1, 2, \dots, n$). Thus when the parameters are determined, the approximated model can be constructed. Similarly to previous estimators, the unknown parameters of $\theta_1, \theta_2, \dots, \theta_n$ are calculated from the formulation as follows:

$$\text{maximize } -\frac{[n_s \ln(\hat{\sigma}^2) + \ln|\mathbf{R}|]}{2} \quad (19)$$

where θ_i ($i=1, 2, \dots, n$) > 0 . In this study, the method of modified feasible direction is utilized to determine the optimum parameters. Finally, Eq. (14) is determined as the explicit form of design variables.

3.3 Design procedures

Step 1: DOE strategy

First of all, the sample points should be set up to obtain the kriging metamodel of weight and maximum stress. DOE

strategies is often used to sample the design space. Depending on analysis time, full combination, orthogonal array or Latin hypercube design can be selected as the sampling method.

Step 2: Matrix experiment

The responses of weight and maximum stress are calculated for each row of the orthogonal array. The number of experiments is identical to the number of rows in orthogonal array. That is, an experiment means one finite element analysis.

Step 3: Building and validation of kriging models

With the responses on the sample points, kriging model of each response is constructed. Therefore, two kriging models are built since the number of responses is two. To assess the kriging model, the error in surrogate model is characterized by using a few metrics. In this research, the metrics defined as Eqs. (20) is utilized¹⁰.

$$CV = \sqrt{\frac{1}{n_s} \sum_{i=1}^{n_s} (f_i - \hat{f}_{-i})^2} \quad (20)$$

where n_s is the number of sample points for validation, and \hat{f}_{-i} is the i -th estimator of kriging model constructed without the i -th observation. In this study, n_s is set up as 10.

The metric CV should construct the kriging models as many as n_s , which is a time consuming process. In Ref. 13), this process is reduced by using the calculated $\hat{\beta}$ and θ , but by calculating \mathbf{R} , \mathbf{r} and \mathbf{f} with respect to n_s-1 sample points. However, this reduction is valid under the assumption that elimination of one sample data has a negligible effect on the maximum likelihood estimates.

Step 4: Optimization using simulated annealing algorithm

Once approximated formulation for optimization is accomplished based on kriging metamodels, a global optimization method such as tabu search method, simulated annealing algorithm or genetic algorithm can be employed to solve the design formulation. In this research, the simulated algorithm is adopted. In the course of calculating the optimum, the computational cost is very low since all the true functions composing optimization formulation are replaced by simple mathematical expressions.

To apply the simulated annealing algorithm, the objective and constraint functions as defined in Eqs. (12)~(13) are combined into a pseudo-objective function. Thus, the formulation for optimization can be reduced as

$$\text{minimize } \phi(t_1, t_2, t_3, l_1) = \mathcal{W} + \alpha \cdot \text{Max}\left[0, (\hat{\sigma}_{\max} - \sigma_a)\right] \quad (21)$$

where α is a positive large number to consider the constraint feasibility of Eq. (13).

Step 5: Convergence criteria

The iterative process would be stopped when the two convergence criteria are satisfied. The two convergence parameters are defined as

$$CP_1 = \frac{|\sigma_{\max}^* - \hat{\sigma}_{\max}^*|}{\sigma_{\max}^*} \times 100 \quad (22)$$

$$CP_2 = CV_{\text{stress}} \quad (23)$$

where $\hat{\sigma}_{\max}^*$ and σ_{\max}^* are the estimated maximum stress and the true stress at the optimum determined from Eq. (21), and CV_{stress}

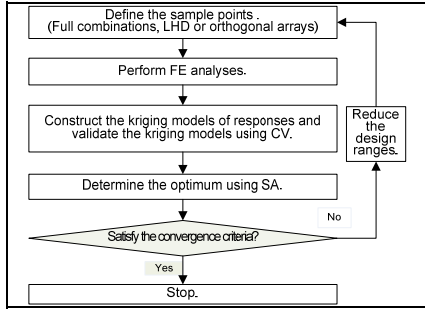


Fig. 7 Suggested design procedures

the CV of maximum stress, respectively. In this research, CP_1 and CP_2 should be less than 3% and 30MPa, respectively.

If any of convergence criteria is satisfied, the design process would be stopped. Otherwise, return to Step 1. Then, for a design variable, the design range between lower and upper bounds is reduced. In this research, its range is fixed as 3mm, referencing the optimum determined from Step 4. If any finite element is distorted in the design range of a design variable, the finite element model should be remeshed. The overall design process is represented in Fig. 7.

4. Results

4.1 Suggested method

The orthogonal array $OA(2,7,49,8)^{14)}$ for Step 1 is utilized. OA means orthogonal array, the numbers in parenthesis represent strength, number of levels, number of rows, and number of columns, from left to right respectively. Since there are four design variables in the jaw design, the last four columns in the arrays are empty. The levels of each design variable are created by discretizing the design space equally. At first iteration, the lower bound is set up as the first level, while the upper bound the last level. The OA that the levels' values are assigned is represented in Table 1. For the Step 2, the calculated responses are summarized in the last two columns of Table 1. The number of FE analyses is 49 since $OA(2,7,49,8)$ is utilized in Step 1.

Based on the responses of weight and maximum stress, the primitive kriging model of each response is constructed by Step 3. The validations of the first kriging models are summarized in Table 2. By Step 4, the optimum is calculated. The predicted and true responses at the optimum are summarized in Table 3, and the convergence criteria at the optimum are listed in Table 4. Since the first kriging models can't satisfy the criteria of Eqs. (22)~(23), the next iteration of design procedures is performed. That is, the levels of design variables are reduced as

$$23.5\text{mm} \leq t_1 \leq 26.5\text{mm} \quad (24)$$

$$27.5\text{mm} \leq t_2 \leq 30.5\text{mm} \quad (25)$$

$$81.0\text{mm} \leq t_3 \leq 84.0\text{mm} \quad (26)$$

$$54.0\text{mm} \leq l_1 \leq 57.0\text{mm}. \quad (27)$$

is

In the second iteration, the orthogonal array $OA(2,7,49,8)$ for Step 1 and the responses are shown as Table 5. From Table 4, it is seen that the optimum determined from the second iteration satisfies the convergence criteria.

Table 1 $OA(2,7,49,8)$ experiments for the 1st iteration

Exp. no.	t_1	t_2	t_3	l_1	w (kg)	σ_{\max} (MPa)
	(mm)					
1	25.0	25.0	75.0	50.0	36.9	747.9
2	25.0	26.7	77.5	53.3	37.5	655.3
⋮	⋮	⋮	⋮	⋮	⋮	⋮
48	35.0	33.3	82.5	53.3	48.1	484.0
49	35.0	35.0	80.0	56.7	47.9	509.9

Table 2 Validations of kriging models for each iteration

Iteration	Response	Optimum parameters				CV
		θ_1	θ_2	θ_3	θ_4	
1	w	0.596	1.295	1.278	0.545	46.5
	σ_{\max}	0.594	1.478	1.465	0.602	
2	w	0.598	1.300	1.281	0.548	23.8
	σ_{\max}	9.762	1.448	1.437	9.770	

Table 3 Optimum results for each iteration

Iter.	Optimum design variables (mm)				Response (σ : MPa, w : kg)			
	t_1	t_2	t_3	l_1	w	w	σ_{\max}	σ_{\max}
1	25.0	29.0	82.5	55.0	38.3	39.6	548.0	560.0
2	23.5	28.4	82.5	55.5	38.2	37.1	542.0	545.2

Table 4 Convergence parameters for each iteration

Iteration	Convergence parameter	
	CP_1	CP_2
1	6.9	46.5
2	2.5	23.8

Table 5 $OA(2,7,49,8)$ experiments for the 2nd iteration

Exp.No.	t_1	t_2	t_3	l_1	w (kg)	σ_{\max} (MPa)
	(mm)					
1	23.5	27.5	81	54	36.8	602.7
2	23.5	28	81.5	55	36.9	541.4
⋮	⋮	⋮	⋮	⋮	⋮	⋮
48	26.5	30	82.5	55	39.98	556.9
49	26.5	30.5	82	56	40.0	576.0

4.2 ANSYS WORKBENCH¹¹⁾

Two methods for shape optimization are built in the software. One is the DOE method, and the other is the VT method. The DOE method in the software adopts the central composite approach as the sampling method and the response surface approach as the approximation method. On the contrary, the VT method utilizes the first-order Taylor series as the approximation method.

Both of them have shortcomings in treating the highly nonlinear functions, even though they have the merit in reducing the computer time to run, since they approximate a true function to linear and quadratic functions, respectively. To supplement

these shortcoming, they supply the three candidate designs. Thus, designer should select the optimum from the candidates. Thus, selecting the optimum design is very intuitive. The

Table 6 Comparisons of results

Methods	Optimum design variables (mm)				Response (σ : MPa, w : kg)			
	t_1	t_2	t_3	l_1	\hat{w}	w	$\hat{\sigma}_{max}$	σ_{max}
DOE	27.0	27.6	81.5	59.0	39.8	39.8	537.6	525.0
VT	28.5	28.5	80.8	51.4	41.5	41.5	535.5	526.9
Suggested method	23.5	28.4	82.5	55.5	38.2	37.1	531.7	545.2

detailed processes are summarized in Ref. 15).

From Table 6, it is seen that the weight of the suggested method is greatly reduced satisfying the constraint, as compared to the DOE and VT methods.

5. Conclusions

The following conclusions can be made from this study.

The present study proposes a structural optimization procedure applicable to jaw design for a container crane based on the kriging approximate models and simulated annealing algorithm. This procedure includes shape optimization, which has been the most difficult to apply in the structural design of a jaw.

Generally, the maximum stress becomes highly nonlinear since its position can be changed with respect to the design point. It is seen that adopting the kriging model to surrogate the maximum stress is efficient. Finally, the approximate maximum stress enables one to solve the formulation for shape optimization with simulated annealing algorithm.

The shape optimum design of a jaw is achieved through kriging approach and global optimization algorithm, considering the severe wind loading conditions. The weight at the optimum is decreased by around 17%, which is more than the optimal solutions of previous study. The results of optimization presented in this paper can apply to the design of another component in a container crane.

Acknowledgement

This work was supported by the Program for the Training of Graduate Students in Regional Innovation which was conducted by the Ministry of Commerce, Industry and Energy of the Korean Government.

Reference

1. [http://www.willis.com/willisre/html/reports/catastrophe/Maemi.pdf#search='typhoon%20maemi%20catastrophe%20report'\(2006\)](http://www.willis.com/willisre/html/reports/catastrophe/Maemi.pdf#search='typhoon%20maemi%20catastrophe%20report'(2006)
2. J. R. Kim, "Wind Resistance Design Learning from Typhoon Maemi," J. of WEIK, Vol. 7, No. 2, pp.150-156, (2003)
3. Ministry of Maritime Affairs & Fisheries, "Management Regulation for Facilities and Equipment in Port," (2004)
4. D. S. Han "A Study on the Structural Design of the Wedge Type Rail Clamp for a Container crane," The Graduate School of Dong-A University in Partial Fulfillment of the Requirements for the Degree of Doctor of Philosophy in Mechanical Engineering (2005)
5. S. W. Lee, J. J. Shim, D. S. Han, J. S. Park, G. J. Han, K. S. Lee, T. H. Kim, "The Effect of Wind Load on the Stability of a Container Crane," J. of KSPE, Vol. 22, No. 2, pp. 148-

- 155, (2005).
6. D. S. Han, G. J. Han, K. H. Lee, and J. M. Lee, "Design of the Various Wedge Type Rail Clamp for Quay Crane according to the Design Wind Speed Criteria Changes," Asia Navigation Conference 2005, pp. 291-301, (2005).
7. Guinta, A. and Watson, L., 1998, "A Comparison of Approximation Modeling Techniques: Polynomial Versus Interpolating Models," Proceedings of the 7th AIAA/USAF/NASA/ISSMO Symposium on Multidisciplinary Analysis and Optimization, St. Louis, Mo, AIAA, Vol. 2, Sep. 2-4, pp. 392-440.(AIAA-98-4758)
8. Sacks, J., Welch, W. J., Mitchell, T. J. and Wynn, H. P., "Design and Analysis of Computer Experiments," Statistical Science, Vol. 4, No. 4, pp.409-435,(1989)
9. Santner, T.J., Williams, B.J. and Notz, W.I., The Design and Analysis of Computer Experiments, Springer, New York, (2003)
10. Lee, K.H., "Optimization of a Driver-Side Airbag Using Kriging Based Approximation Model," Journal of Mechanical Science and Technology, Vol. 19, No. 1, pp. 116-126,(2005)
11. "ANSYS WORKBENCH Training Manual" Taesung software&engineering.inc
12. BS2573, British Standards UK.
13. Jones, D.R., Schonlau, M. and Welch, W.J., "Efficient Global Optimization of Expensive Black-Box Functions," Journal of Global Optimization, Vol. 13, No. 4, pp,(1998)
14. Sherwood, G, (2006) <http://home.att.net/~gsherwood/cover.htm>.
15. I. K. Bang, D. H. Kang, D. S. Han, G. J. Han, K. H. Lee, " Shape Optimization for a Jaw Using Design Of Experiments" Submitted to KINPR (2006)